Design and Implementation of Model Parameter Independent Robust Current Control Scheme of Three-Phase Inverter - A Neural Network-Based Classification Approach

Machina Venkata Siva PRASAD, Koduru Sriranga SUPRABHATH, Sreedhar MADICHETTY, Sukumar MISHRA, and Abdelkader EL KAMEL

***Abstract*—In recent years, there has been a notable surge of interest in integrating advanced control techniques within power electronic systems. This article presents the utilization of neural network (NN) controllers within the realm of three-phase inverter control. While traditional control methods like proportional integral-derivative (PID) and pulse width modulation (PWM) have proven effective, they sometimes fall short of meeting the demands of modern applications. These contemporary requirements encompass heightened precision, adaptability to changing conditions, and resilience against uncertainties. This study employs an NN controller to achieve current control in a three-phase standalone inverter system. A dataset is prepared using model predictive control (MPC) to train the neural network model, and appropriate hyperparameters are chosen, facilitating offline learning. The entire setup is implemented within the MATLAB Simulink platform, allowing for an in-depth analysis of its performance. This analysis includes the assessment of prediction errors and the evaluation of total harmonic distortion (THD). In addition, the article conducts a comparative study between the neural network controller and the MPC controller, presenting and discussing the obtained results. Further, the proposed method is realized in the hardware in loop OPAL - RT setup, and the real-time performance is analyzed.**

***Index Terms*—Backpropagation, multi-class classification, model predictive control, neural network control, three-phase inverter.**

I. Introduction

CLOSED-loop control of inverters is pivotal in various applications, encompassing motor drives, renewable energy systems, uninterruptible power supplies (UPS), and similar domains. This control approach involves continuous monitoring of the inverter system's output and feedback, facilitating immediate adjustments to maintain the desired operational parameters. Inverter closed-loop control achieves precise voltage and frequency regulation, enhances system stability, and delivers superior transient performance. It also proves invaluable in optimizing motor control, mitigating harmonic distortions, and dynamically responding to changing conditions.

Numerous control strategies have been proposed in the literature. These range from classical control techniques like hysteresis control [1], [2], linear control [3], [4], and proportional integral-derivative (PID) control [5], [6], to advanced control approaches such as fuzzy logic control [7], sliding mode control [8], and predictive strategies like deadbeat predictive control [9], [10], as well as model predictive control (MPC) strategies [11], [12].

The evolution of artificial neural networks has simplified the control of complex power electronic systems. Neural network's (NN's) ability to generalize and adapt to unforeseen scenarios makes it a favorable choice for controlling power electronic converters.

The utilization of power electronic converters has expanded its reach across various domains, including electric vehicles, renewable energy systems, power system control, battery chargers, electric traction, microgrids, and numerous others. Given the wide and diverse array of applications, a need arises for control algorithms that can effectively operate across this spectrum of real-world scenarios. Traditional control mechanisms, which rely on mathematical models and deterministic approaches, contribute to increased complexity in design. Moreover, these traditional methods are fundamentally linear, assuming linearity in system operations. Consequently, when dealing with non-linear systems, these control methods necessitate numerous assumptions, resulting in performance that may be inaccurate and inefficient.

Hence, there arises a requirement for a universal control mechanism capable of offering generalized solutions for diverse applications. Such a control mechanism should also exhibit high adaptability in the face of challenging and adverse scenarios. This is where artificial intelligence techniques, particularly neural networks come into play as a viable solution to address the limitations of traditional

Manuscript received October 1, 2023; revised December 9, 2023; accepted December 19, 2023. Date of publication June 30, 2024; date of current version January 2, 2024. This work was supported in part by Department of Science and Technology for Social Development under grant DST/TMD/SERI/RES/2020/27. (*Corresponding author: Sreedhar Madichetty*.)

M. V. S. Prasad and S. Madichetty are with the Ecole Centrale School of Engineering, Mahindra University, Hyderabad, Telangana 500043, India (e-mail: mvspchowdary@gmail.com; sreedhar.803@gmail.com).

K. S. Suprabhath and S. Mishra are with the Indian Institute of Technology (ISM) Dhanbad, Dhanbad, Jharkhand 826004, India (e-mail: srirangakoduru@gmail.com; sukumarmiitdelhi@gmail.com).

A. EL KAMEL is with Centrale Lille, Centrale Lille Institute, Villeneuve-d'Ascq, Hauts-de-France 59651, France (e-mail: abdelkader.elkamel@centralelille.fr).

Digital Object Identifier 10.24295/CPSSTPEA.2023.00052

methods. Neural networks, renowned as universal predictors, possess remarkable adaptability and generalization capacity, particularly in nonlinear systems.

II. Literature Review

In literature, control mechanisms are traditionally divided into three categories: classical control methods, advanced control methods, and intelligent control methods. Among classical control methods, hysteresis and linear control are the most popular. [13] discusses various hysteresis control mechanisms such as single-band hysteresis, double-band hysteresis, modified double-band hysteresis, and variable-band hysteresis control methods. To increase the performance of the inverter by obtaining less total harmonic distortion (THD) and for maximum switching frequencies, these variants of hysteresis control are designed. However, implementing hysteresis control involves high switching losses and high electromagnetic interference. Also, the fixed hysteresis band limits the application's precision and generates heavy oscillations in switching states. Current mode PI controllers are designed in [14], where the feedback currents are compared with the reference values and passed through the PI controller to generate the control variable. Further, the output is processed in the modulation stage to generate the appropriate switching signals. In this method, tuning of PI controller parameters decides the transient and steady-state behavior. Tuning these parameters proves difficult for nonlinear systems; using advanced methodologies for parameter tuning increases the design complexity. Space vector modulation (SVM) is another popular control used in industries; this method performs better than pulse width modulation techniques in harmonic performance. [15], uses SVM for achieving soft switching in three-phase inverters. Although this method is inherently non-linear and performs better for nonlinear systems, the high computational overhead and high sensitivity towards parameter variations limit its applications. A sliding mode control mechanism is introduced to improve the performance of non-linear and highly dynamic systems. [16] discusses implementing sliding mode control for the multilevel inverter. This control algorithm develops a sliding mode theory to evaluate cost functions and optimize the control input. Although this method is very robust compared to its counterparts, it introduces the chattering problem, leading to high-frequency oscillations near the sliding boundary [17], [18]. Also, this method is proved to be highly sensitive towards parameter variations. As a part of advanced control strategies, MPC techniques have been used lately. Based on the requirement of modulation stages, they are categorized as modulation-based and modulation-free predictive controls [19]. A shared underlying principle in all predictive control techniques is their reliance on the dynamic system model to forecast the plant's future performance. They then execute optimal control actions based on pre-established control objectives [20]. [21] discusses optimized switching sequences with finite control set MPC in voltage source inverters. MPCs are constantly evolving based on their applications; the predictive ability and a systematic approach to obtaining a solution make them widely acceptable in industries. However, the major disadvantage of using MPC is its designing stage; the design of MPC includes modeling of the system. It also increases the computational complexity as it requires solving optimization problems in every step. High computational complexity, tuning complexity, and inaccurate error modeling are some of the limitations of MPC.

The above studies show that although MPC and its variants are proven to be very efficient compared to traditional control methodologies, there is a need to reduce the complexity of designing and implementing. Therefore, a neural network-based control mechanism is developed to control the three-phase standalone inverter in this article.

Further, this article is arranged as follows: Section III details the proposed methodology with mathematical modeling of inverter control, workflow comparison between MPC and NN control, and a detailed explanation of the design of the NN controller. Section IV presents the result analysis, where the operation of the NN controller is observed with simulation results. Subsequently, the performance of MPC and NN controllers is compared with various performance measures. This article concludes in Section V, stating the performance efficiency of the proposed model and discussing future scope in the NN control domain.

III. Proposed Methodology

A. Three-Phase 2 level Inverter

The conventional approach for operating a three-phase, 2 level inverter with MPC has been the predominant method used in research for implementing closedloop inverter operation [22]. This article introduces a novel approach to neural network-based closed-loop control for the inverter. Fig. 1 illustrates the fundamental schematic distinctions between the MPC and the proposed methods. The workflow divergence between MPC and the proposed NN model is depicted in the flowchart presented in Fig. 2.

B. Neural Network Control

The fundamental architecture of a neural network consists of an input layer, multiple hidden layers, and an output layer. Neural networks serve a dual purpose: they can predict a single value, referred to as regression, and they can also classify input features into distinct classes, known as classification. Unlike regression, classification involves a predetermined set of output classes. Therefore, any inputs provided to the neural network model must yield outcomes within the predefined categories of the output classes.

In the context of classification, neural networks are often used for multi-class classification. In this technique, the output nodes provide probabilistic outputs for each of the distinct classes, allowing for the assessment of the likelihood of an input belonging to each class.

The workflow for multi-class classification using an NN is illustrated in Fig. 3. The process begins with data collection and subsequently involves preprocessing to ensure uniformity, as outlined in (1). Next, the input and output data are imported.

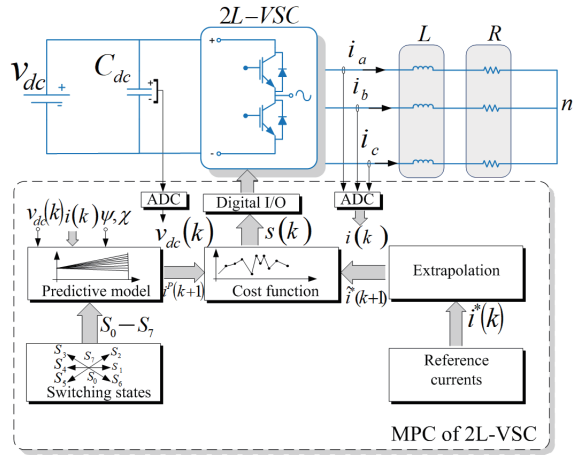

(a)

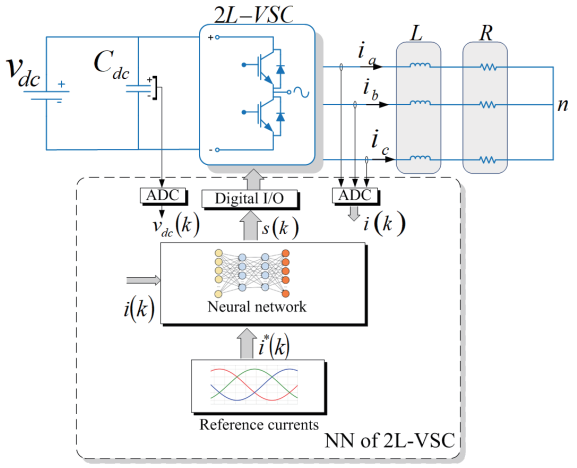

(b)

Fig. 1. (a) Conventional MPC for inverter three–phase 2, level inverter and (b) proposed NN model for closed loop operation of three–phase 2, level inverter.

The dataset is divided into training, testing and validation sets.

A defined NN model allows for user-specified hidden layer nodes, which may incorporate various activation functions like sigmoid and rectified linear unit (ReLU), as indicated in (2). However, a specific activation function, softmax, is used for the output layer, which will be further discussed in subsequent sections.

$$x^{i}_{\text{scaled}} = \frac{x^{(i)} - x_{\min}}{x_{\max} - x_{\min}} \tag{1}$$

Here x^{i}_{scaled} is an input feature of the sample space.

$$\begin{cases} Sigmoid(x) = \dfrac{1}{e-x} \\ ReLU(x) = \begin{cases} 0 \text{ for } x \leqslant 0 \\ x \text{ for } x > 0 \end{cases} \end{cases} \tag{2}$$

After defining the model, the weight parameters are trained through the backpropagation process. Cross-entropy is employed to calculate the error during this training phase. Once the model is successfully trained on the training dataset, it is then

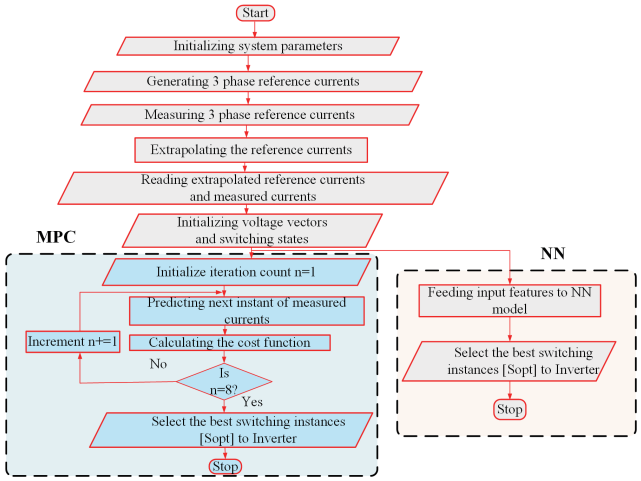

Fig. 2. Workflow comparison between MPC control and NN control.

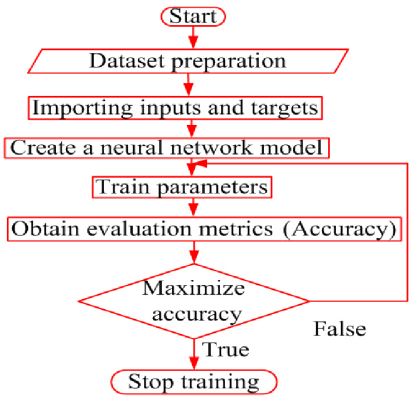

Fig. 3. Flow chart for multi-class classification.

evaluated using the separate test and validation datasets. Fig. 4 illustrates a sample neural network model utilized for multi-class classification. In the sample schematic, the NN model consists of one input layer followed by two hidden layers with one output layer. Here $[x_1, x_2, \cdots, x_D]$ are the input samples considered. The first hidden layer nodes are given by $[A_{11}, A_{12}, \cdots, A_{1P}]$, the second hidden layer nodes are given by $[A_{21}, A_{22}, \cdots, A_{2Q}]$. The output layer nodes are depicted by $[N_1, N_2, \cdots, N_H]$. In short, the model can be conveyed as *D–P–Q–H*. The bias terms (B_1, B_2, B_3) are the bias units for the first hidden layer, second hidden layer, and output layer, respectively. The weight matrix between the input layer and the first hidden layer is represented by $W_x^{A_1}$ and given in (3).

$$W_x^{A_1} = \begin{bmatrix} W_{B_1A_{11}} & W_{B_1A_{12}} & \cdots & W_{B_1A_{1P}} \\ W_{x_1A_{11}} & W_{x_1A_{12}} & \cdots & W_{x_1A_{1P}} \\ W_{x_2A_{11}} & W_{x_2A_{12}} & \cdots & W_{x_2A_{1P}} \\ \vdots & \vdots & \ddots & \vdots \\ W_{x_DA_{11}} & W_{x_DA_{12}} & \cdots & W_{x_DA_{1P}} \end{bmatrix} \tag{3}$$

Here $W_{B_1A_{11}}$ represents the weight between bias term B_1 and first node of first hidden layer A_{11} and $W_{x_1A_{11}}$ represents the

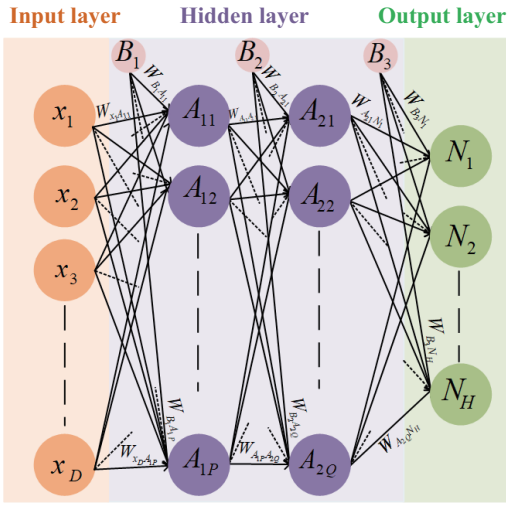

Fig. 4. Sample NN model for multi-class classification.

weight between first input layer node and first hidden layer node A_{11} respectively and the rest of the weights will follow in same manner.

The weight matrix between the first hidden layer and the second hidden layer is depicted by $W_{A_1}^{A_2}$ and given in (4). Similarly, The weight matrix between the second hidden layer and the output layer is depicted by $W_{A_1}^{N}$ and given in (5).

$$W_{A_1}^{A_2} = \begin{bmatrix} W_{B_2A_{21}} & W_{B_2A_{22}} & \cdots & W_{B_2A_{2Q}} \\ W_{A_{11}A_{21}} & W_{A_{11}A_{22}} & \cdots & W_{A_{11}A_{2Q}} \\ W_{A_{12}A_{21}} & W_{A_{12}A_{22}} & \cdots & W_{A_{12}A_{1Q}} \\ \vdots & \vdots & \ddots & \vdots \\ W_{A_{1P}A_{21}} & W_{A_{1P}A_{22}} & \cdots & W_{A_{1P}A_{2Q}} \end{bmatrix} \tag{4}$$

$$W_{A_2}^{N} = \begin{bmatrix} W_{B_3N_1} & W_{B_3N_2} & \cdots & W_{B_3N_H} \\ W_{A_{21}N_1} & W_{A_{21}N_2} & \cdots & W_{A_{21}N_H} \\ W_{A_{22}N_1} & W_{A_{22}N_2} & \cdots & W_{A_{22}N_H} \\ \vdots & \vdots & \ddots & \vdots \\ W_{A_{2Q}N_1} & W_{A_{2Q}N_2} & \cdots & W_{A_{2Q}N_H} \end{bmatrix} \tag{5}$$

The output layer of the NN model is shown in Fig. 5, where a single node is represented, and its working is given in (6).

$$\begin{cases} Z_1 = \sum_{i=1}^{Q} gA_{2i} * W_{A2iN1} + W_{B3}N_1 \\ O_1 = S(Z_1) \end{cases} \tag{6}$$

Here $g_{A_{2i}}$ refers to the outputs of hidden layer two neurons, where (i = 1, 2, 3, · · · ,Q) and $W_{A_{2i}N_1}$ is the weight vector between hidden layer 2 neurons and output node N_1. The softmax $S(Z_i)$ activation function is given in (7) and (8).

$$S(Z_i) = \frac{e^{Z_i}}{\sum_{i=1}^{N} e^{Z_i}} \tag{7}$$

where $S(Z_i) = O_i$.

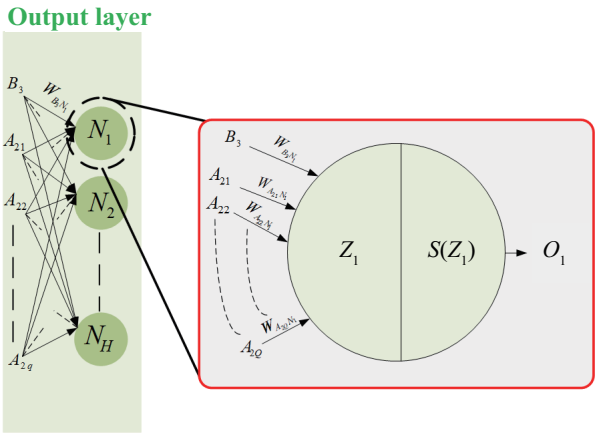

Fig. 5. Output layer of multi-class classification.

$$\sum_{i=1}^{H} O_i = 1 \tag{8}$$

Here (O_1,O_2,O_3, ⋯ ,O_H) are the predicted outputs where as (y_1, y_2, y_3, ⋯ , y_H) are the ground truths or the actual values. A single node's cross-entropy error value is given in (9).

$$e_H = -y_H \times \ln(O_H) \tag{9}$$

The total error E is given in (10).

$$E = \sum_{i=1}^{H} e_i \tag{10}$$

Substituting (9) in (10) to obtain (11).

$$E = -\sum_{i=1}^{H} y_i \times \ln(O_i) \tag{11}$$

Computing gradients that are required for backpropagation, which uses a gradient descent algorithm to update the parameters of NN as shown in (12) and (13).

$$\frac{\partial E}{\partial Z_k} = \frac{\partial\left[-\sum_{i=1}^{H} y_i \times \ln(O_i)\right]}{\partial Z_k} \tag{12}$$

$$\frac{\partial E}{\partial Z_k} = -\sum_{i=1}^{H} \frac{\partial y_i \times \ln(O_i)}{\partial Z_k} \tag{13}$$

Since y_i is independent of Z_k, which is the input of softmax activation function. The above equation is re-written as (14).

$$\frac{\partial E}{\partial Z_k} = -\sum_{i=1}^{H} y_i \times \frac{\partial \ln(O_i)}{\partial Z_k} \tag{14}$$

Since O_i is not a direct function of Z_k. The chain rule is applied as shown in (15)

$$\frac{\partial \ln(O_i)}{\partial Z_k} = \left[\frac{\partial ln(O_i)}{\partial O_i} \times \frac{\partial O_i}{\partial Z_k}\right] \tag{15}$$

Substituting (15) in (14), we get (16)

TABLE I
SPECIFICATIONS OF THREE-PHASE TWO-LEVEL INVERTER

Parameter	Value
Input voltage	520 V
Resistance	10 Ω
Inductance	10 mH
Sampling time	1 μs
Reference current	10 A

$$\frac{\partial E}{\partial Z_k} = -\sum_{i=1}^{H} y_i \times \left[\frac{\partial \ln(O_i)}{\partial O_i} \times \frac{\partial O_i}{\partial Z_k}\right] \tag{16}$$

Substituting $\frac{\partial \ln(O_i)}{\partial O_i} = \frac{1}{O_i}$ in (16) to obtain (17).

$$\frac{\partial E}{\partial Z_k} = -\sum_{i=1}^{H} \left(\frac{y_i}{O_i} \times \frac{\partial O_i}{\partial Z_k}\right) \tag{17}$$

The partial derivative of the softmax function is given in (18).

$$\frac{\partial O_i}{\partial Z_k} = \begin{cases} O_i \times (1 - O_i) & \text{if } i = k \\ -O_i \times O_k & \text{if } i \neq k \end{cases} \tag{18}$$

Substituting (18) in (17), we obtain (19).

$$\frac{\partial E}{\partial Z_k} = -\sum_{i \neq k}^{H} \left\{\left(\frac{y_i}{O_i} \times -O_i \times O_k\right) + \left[\frac{y_i}{O_k} \times O_k \times (1 - O_k)\right]\right\} \tag{19}$$

Here (19) is simplified into (20) and (21)

$$\frac{\partial E}{\partial Z_k} = -\sum_{i \neq k}^{H} \left\{(-y_i \times O_k) + \left[y_k \times (1 - O_k)\right]\right\} \tag{20}$$

$$\frac{\partial E}{\partial Z_k} = -\left\{\left(-O_k \times \sum_{i \neq k}^{H} y_i\right) + \left[y_k \times (1 - O_k)\right]\right\} \tag{21}$$

Further, (21) can be simplified as (24) using (22) and (23).

$$\sum_{i=1}^{H} y_i = 1 \tag{22}$$

$$\sum_{i \neq k}^{H} y_i = \sum_{i=1}^{H} y_i - y_k = 1 - y_k \tag{23}$$

$$\frac{\partial E}{\partial Z_k} = \left[(O_k(1 - y_k)\right] - \left[y_k \times (1 - O_k)\right] \tag{24}$$

After simplification of (24), the error gradient is given in (25).

$$\frac{\partial E}{\partial Z_k} = O_k - y_k \tag{25}$$

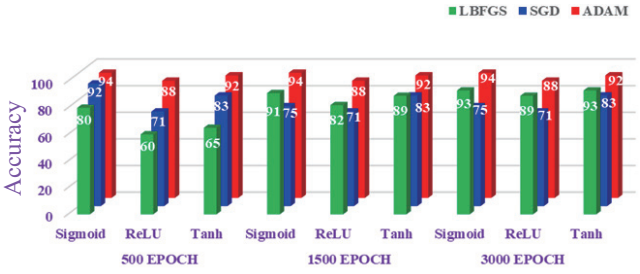

Fig. 6. Different accuracy scores of multi-class classification with multiple parameters changes.

IV. RESULTS

A neural network controller is developed to control the three-phase inverter's current control. The design and implementation of the NN controller are performed in the MATLAB Simulink platform. Specifications of the inverter model considered for the study are given in Table II. Initially, a three-phase inverter with MPC control is implemented, and the data is collected from the system. The dataset for training consists of three-phase measured currents as input features and the switching states as output. Once the data is collected, the NN model is trained with various combinations of hyperparameters such as epochs, activation functions, and optimizers. Each combination performs differently, providing different accuracies in prediction, as shown in Fig. 6. The combination with the highest accuracy is selected to obtain the optimized switching sequence, which is an Adam optimizer with a sigmoid activation function for 500 epochs. The inverter is controlled to operate at reference currents of 10 A. The efficiency of the NN controller can be examined by overlapping the reference currents and measured currents for each phase individually. Further, the operation of the NN controller with different scenarios, such as reference changes and parametric changes is explored.

A. Reference Change

To examine the adaptability and robustness of the designed control scheme, the reference value is varied at 0.5 s from 10 A to 5 A as shown in Fig. 7. By analyzing Figs. 8 and 9, it can be understood that the designed controller performs efficiently and adapts to the system changes. Fig. 10 denotes the switching instances generated by the NN controller; it is observed that the NN controller takes 0.0001 s to adapt to the new reference value.

B. Parametric Variations

As we have seen, traditional control methods are often sensitive to parametric changes; predictive and intelligent techniques are used to overcome that. In this case, load change is performed by varying inductance and resistance values, and the errors in predictions are analyzed for both MPC and NN.

1) Resistance variation: In this case, input DC voltage is maintained at 520 V, inductance is maintained constant at 10 mH, but the resistance value varies from 5 Ω to 30 Ω. Fig. 11

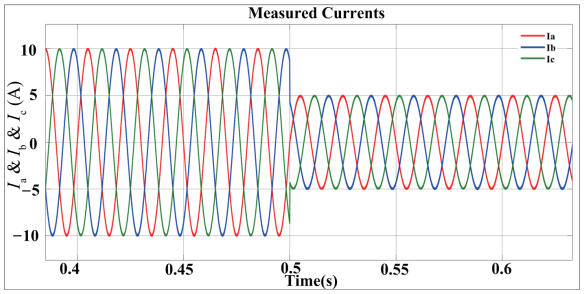

Fig. 7. Measured output currents of three-phase inverter with reference change.

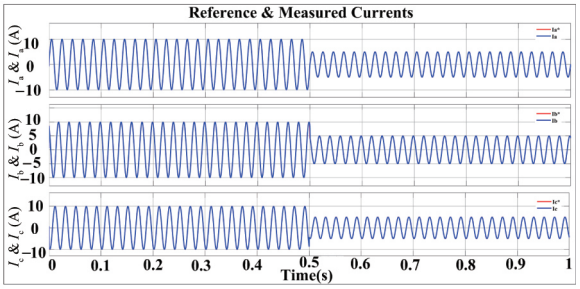

Fig. 8. Reference currents and measured currents of three-phase inverter with reference change.

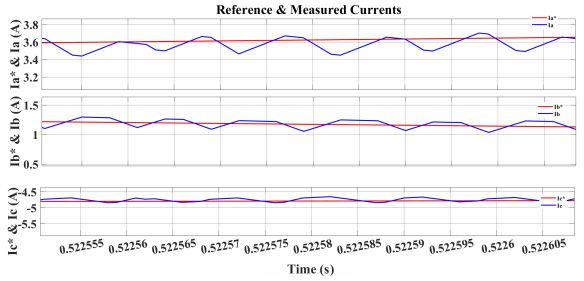

Fig. 9. Zoomed version of reference currents and measured currents of three-phase inverter with reference change.

indicates the prediction error obtained during resistance change, including the maximum error and minimum error in each phase prediction. It can be observed from Fig. 11 that the error in prediction in the MPC controller increases gradually as the change in resistance value increases. However, the error in NN controller prediction is much less and almost constant for any change in resistance.

2) Inductance variation: The inductance value varies from 1 mH to 30 mH, keeping the resistance value and input voltage constant at 10 Ω and 520 V , respectively. Fig. 12 shows the minimum and maximum errors for each phase in MPC control and NN control. It can be inferred from Fig. 12 that as the inductance value increases, the prediction error is reduced for both MPC and NN controllers. It shows that the inductance variation will not have much effect on the prediction.

Therefore, from the above case studies, the NN controller is highly adaptable to system changes and is not sensitive toparametric changes. This makes the NN controller more robust and reliable in dynamic operating conditions.

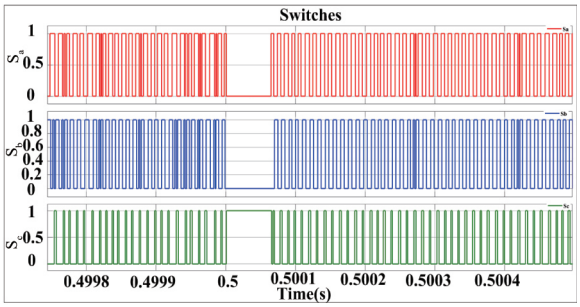

Fig. 10. Switching pulses during reference change.

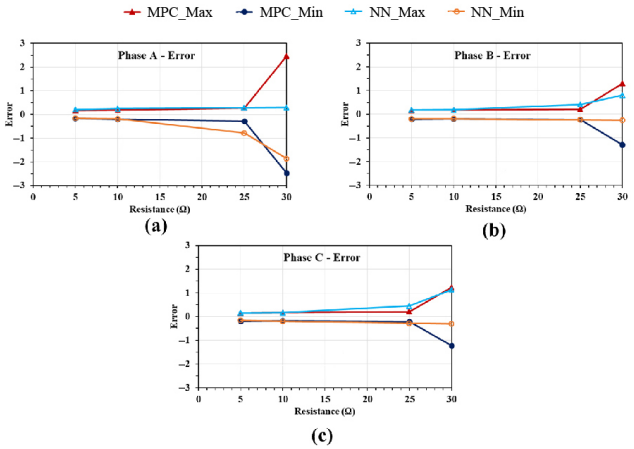

Fig. 11. Error comparison for MPC and NN controller during resistance variations.

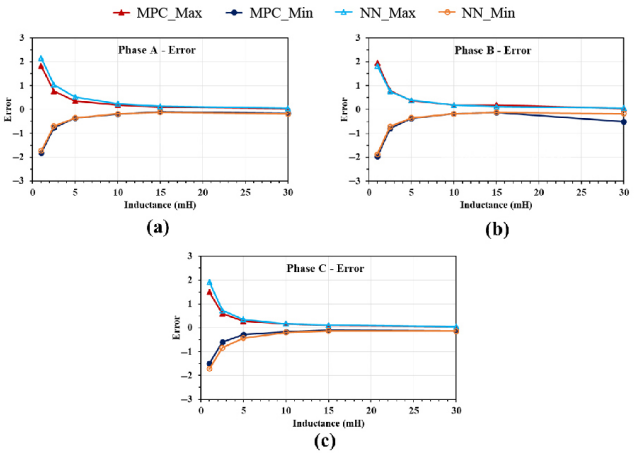

Fig. 12. Error comparison for MPC and NN controller during inductance variations.

C. THD Evaluation

One of the quality measures for the inverter output is the calculation of THD. Ideally, the output of the inverter should consist of only fundamental frequencies. Other than fundamental frequencies, it indicates the distortions in the current waveform. As reference currents are the simulated

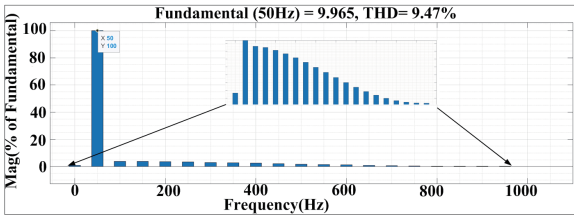

Fig. 13. FFT response of MPC controller.

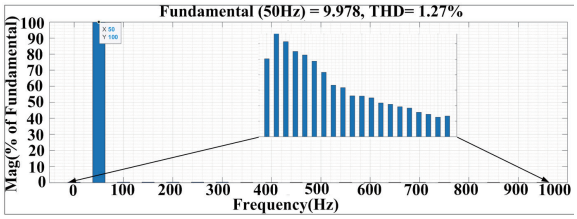

Fig. 14. FFT response of NN controller.

TABLE II
COMPARISON BETWEEN SWITCHING FREQUENCY AND THD

Control method	Switching frequency range / kHz	THD / %
MPC	95–125	9.47
ANN	130–161	1.27

waveforms, it is expected to be 100 % fundamental component. Further, MPC control and NN control are implemented, and their fast Fourier transform (FFT) response is analyzed. Figs. 13 and 14 show the FFT responses of MPC control and NN control, respectively. It can be seen that the THD for NN control is 1.27 % and MPC control is 9.47 %. Zoomed versions in the figures represent the presence of other frequency components with very little percentage. Reduction in THD leads to increased switching frequency. Table III explains the relation between THD and switching frequency obtained for MPC and ANN controllers. It can be observed that the switching frequency range of the ANN controller is a little high compared to MPC, but there is a significant reduction in THD that improves the power quality. Therefore, there should be a tradeoff between THD and switching frequency, where the ANN controller is effective in this case.

The stability of the closed loop operation of the system can be understood by examining the bode plot for the system. Fig. 15 indicates the bode plot of the ANN-controlled inverter with a bandwidth of 160 Hz, indicating that the system gives a stable response without any magnitude attenuation till 160 Hz.

D. Hardware Results

The proposed ANN controller for the three-phase standalone inverter is realized in the hardware in-loop setup of OPAL-RT. Three-phase inverter is connected to a 400 V DC bus controlled with the current command. The trained ANN model can be deployed into the basic microcontrollers using the MATLAB Simulink platform. MATLAB provides hardware supported

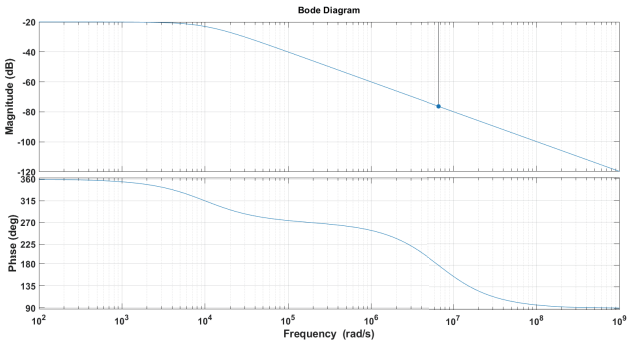

Fig. 15. Bode plot for ANN controlled inverter.

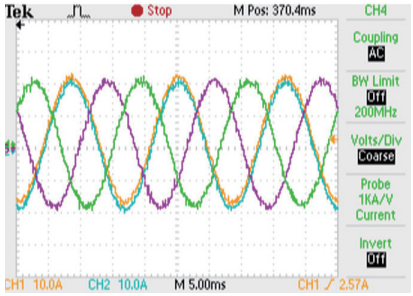

Fig. 16. Reference currents and measured currents with NN controller.

packages for multiple microcontrollers. The trained neural network is deployed into the ATSAM3X8E microcontroller in this work. It is observed that the space occupied by the ANN model is 23 kB with an execution time of 0.1 µs. Therefore, the offline trained neural network can be converted into the hardware-supported file and deployed into the basic microcontroller. This gives the flexibility to attain robust control with minimal computational resources. NN controlled three–phase inverter is controlled with reference currents of 10 A peak–to–peak amplitude. Fig. 16 shows that the proposed control scheme operates precisely by tracking the reference currents accurately. The zoomed version of the waveform is presented in Fig. 17. It can be observed that the error between the reference and the actual waveform is much less as obtained in simulations.

Reference current amplitude is changed from 8 A peak to peak to 20 A in Fig. 18 to verify the robustness of the ANN controller. CH1 and CH2 denote the reference current enotes and measured currents, respectively. It can be seen that the NN controller adjusts to reference change and facilitates a smooth transition.

V. CONCLUSION

This article has explored integrating advanced control techniques, specifically neural network (NN) controllers, within the domain of three-phase inverter control. The study presented in this article successfully demonstrated the application of an NN controller for achieving precise current control in a three-phase standalone inverter system. This approach utilized a

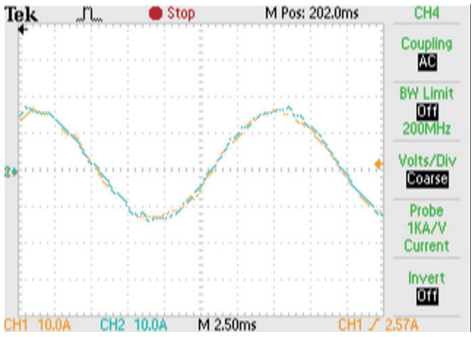

Fig. 17. Reference tracking with NN controller.

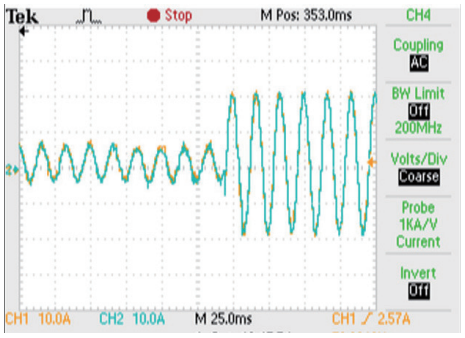

Fig. 18. Reference and measured currents during reference change.

dataset generated by model predictive control (MPC) for training. It selected appropriate hyperparameters to enable offline learning, showcasing its adaptability and optimization capabilities in varying operational conditions.

The robust MATLAB Simulink platform provided an ideal environment for comprehensively analyzing the NN controller's performance. This analysis included a detailed examination of prediction errors and an evaluation of total harmonic distortion (THD), both of which are critical metrics for assessing the controller's effectiveness in maintaining system stability and output quality. Moreover, this article contributes significantly to the field by comparing the newly introduced neural network controller and the established MPC controller. The results presentation and discussion shed light on each approach's strengths and weaknesses, providing valuable insights into their applicability across various real-world scenarios.

Adopting neural network controllers in three-phase inverter systems represents a substantial advancement toward realizing more intelligent and adaptable power electronic systems. As technology continues to evolve and application requirements become increasingly complex, these innovative control techniques promise to meet and surpass the expectations of modern power electronics. This study is a pivotal step in unlocking the full potential of neural networks in the domain of power electronic control, encouraging further exploration and refinement of these methodologies in future research and industrial applications.

References

[1] C. Jaen, J. Pou, R. Pindado, V. Sala, and J. Zaragoza, "A linearquadratic regulator with integral action applied to PWM dc-dc converters," in *Proceedings of IECON 2006-32nd Annual Conference on IEEE Industrial Electronics*, 2006, pp. 2280–2285.

[2] B. K. Bose, *Power Electronics and Motor Drives: Advances and Trends, Second Edition*, Academic Press, 2010.

[3] M. A. Hossain, M. Azim, M. Mahmud, and H. Pota, "Primary voltage control of a single-phase inverter using linear quadratic regulator with integrator," in *Proceedings of 2015 Australasian Universities Power Engineering Conference (AUPEC)*, 2015, pp. 1–6.

[4] K. H. Ahmed, A. M. Massoud, S. J. Finney, and B. W. Williams, "Optimum selection of state feedback variables PWM inverters control," in *Proceedings of 2008 4th IET Conference on Power Electronics, Machines and Drives*, York, 2008, pp. 125–129.

[5] J. Miret, A. Camacho, M. Castilla, L. G. de Vicuña, and J. Matas, "Control scheme with voltage support capability for distributed generation inverters under voltage sags," in *IEEE Transactions on Power Electronics*, vol. 28, no. 11, pp. 5252–5262, Nov. 2013.

[6] Z. Liu, J. Liu, and Y. Zhao, "A unified control strategy for threephase inverter in distributed generation," in *IEEE Transactions on Power Electronics*, vol. 29, no. 3, pp. 1176–1191, 2013.

[7] M. A. Hannan, Z. A. Ghani, M. M. Hoque, P. J. Ker, A. Hussain, and A. Mohamed, "Fuzzy logic inverter controller in photo voltaic applications: Issues and recommendations," in *IEEE Access*, vol. 7, pp. 24934–24955, 2019.

[8] J. Y. Hung, W. Gao, and J. C. Hung, "Variable structure control: A survey," in *IEEE Transactions on Industrial Electronics*, vol. 40, no. 1, pp. 2–22, Feb. 1993.

[9] S. Tahir, J. Wang, G. S. Kaloi, and M. H. Baloch, "Robust digital deadbeat control design technique for 3 phase VSI with disturbance observer," in *IEICE Electronics Express*, vol. 14, no. 13, pp. 20170351–20170351, 2017.

[10] J. Kim, J. Hong, and H. Kim, "Improved direct deadbeat voltage control with an actively damped inductor-capacitor plant model in an islanded AC microgrid," in *Energies*, vol. 9, no. 11, p. 978, 2016.

[11] J. Hu, J. Zhu, and D. G. Dorrell, "Model predictive control of grid-connected inverters for PV systems with flexible power regulation and switching frequency reduction," in *IEEE Transactions on Industry Applications*, vol. 51, no. 1, pp. 587–594, Jan.-Feb. 2015.

[12] T. Sathiyanarayanan and S. Mishra, "Synchronous reference frame theory based model predictive control for grid connected photovoltaic systems," in *IFAC-Papers On Line*, vol. 49, no. 1, pp. 766–771, 2016.

[13] J. K. Singh and R. K. Behera, "Hysteresis current controllers for grid connected inverter: Review and experimental implementation," in *Proceedings of 2018 IEEE International Conference on Power Electronics, Drives and Energy Systems (PEDES)*, 2018, pp. 1–6.

[14] S. Cherati, N. Azli, S. Ayob, and A. Mortezaei, "Design of a current mode PI controller for a single-phase PWM inverter," in *Proceedings of 2011 IEEE Applied Power Electronics Colloquium (IAPEC)*, 2011, pp. 180–184.

[15] Y. Wu, N. He, M. Chen, and D. Xu, "Generalized space-vectormodulation method for soft-switching three-phase inverters," in *IEEE Transactions on Power Electronics*, vol. 36, no. 5, pp. 6030–6045, May 2020.

[16] H. Makhamreh, M. Trabelsi, O. Kükrer, and H. Abu-Rub, "An effective sliding mode control design for a grid-Connected PUC7 multilevel inverter," in *IEEE Transactions on Industrial Electronics*, vol. 67, no. 5, pp. 3717–3725, May 2020.

[17] H. Athari, M. Niroomand, and M. Ataei, "Review and classification of control systems in grid-tied inverters," in *Renewable and Sustainable Energy Reviews*, vol. 72, pp. 1167–1176, 2017.

[18] M. Niroomand and H. Karshenas, "Hybrid learning control strategy for three-phase uninterruptible power supply," in *IET Power Electronics*, vol. 4, no. 7, pp. 799–807, Sept. 2011.

[19] P. Karamanakos, E. Liegmann, T. Geyer, and R. Kennel, "Model predic-

tive control of power electronic systems: Methods, results, and challenges," in *IEEE Open Journal of Industry Applications*, vol. 1, pp. 95–114, 2020.

[20] A. Linder, R. Kanchan, P. Stolze, and R. Kennel, *Model-based Predictive Control of Electric Drives*, Cuvillier Verlag, 2010. [Online]. Available:https://cuvillier.de/uploads/preview/public_file/1590/9783869553986.pdf

[21] C. Zheng, T. Dragičević, Z. Zhang, J. Rodriguez, and F. Blaabjerg, "Model predictive control of LC-filtered voltage source inverters with optimal switching sequence," in *IEEE Transactions on Power Electronics*, vol. 36, no. 3, pp. 3422–3436, Mar. 2021.

[22] V. Yaramasu and B. Wu, *Model Predictive Control of Wind Energy Conversion Systems*, John Wiley & Sons, 2017.

Machina Venkata Siva Prasad received the B.Tech. degree in Electronics and Communication Engineering from the Anna University, Chennai, India, in 2016. M.Tech. in Digital Electronics and Communication Systems from Jawaharlal Nehru Technological University, Anantapur, Anantapuramu, India, in 2019. He is currently working towards a Ph.D. degree in the area of cyber-physical systems and power electronics at the Department of Electronics and Computer Engineering, Mahindra University, Hyderabad, India. His current research interests include the application of artificial intelligence in power electronics and cyber-physical systems.

Koduru Sriranga Suprabhath earned his B.Tech. in Electrical and Electronics Engineering from GITAM University, Hyderabad, India, in 2016. He pursued an M.Tech. in Power Systems from Jawaharlal Nehru Technological University, Hyderabad, India, graduating in 2019. In 2020, he completed his Ph.D. in Cyber-Physical Systems and Power Electronics at the Department of Electronics and Computer Engineering, Mahindra University, Hyderabad, India. He worked as a Research Assistant at IIT Delhi. Presently, he serves as a SERB Sponsored NPDF at IIT(ISM) Dhanbad. His research focuses on artificial intelligence applications in power electronics and cyber-physical systems modeling.

Sreedhar Madichetty earned his B.Tech. in Electrical and Electronics Engineering from Jawaharlal Nehru Technological University, Anantapur in 2010, and his M.Tech. in Power Electronics and Drives (Topper and Gold Medal) and Ph.D. in Power Electronics from KIIT University in 2012 and 2015, respectively. He joined BITS Pilani as a Lecturer in 2014, then became an SERB NPDF at IIT Delhi in 2017, and a Senior Research Fellow at Trinity College Dublin in 2019. Currently, he is an Associate Professor at Ecole Centrale, Mahindra University, Hyderabad. He has authored over 50 research articles, focusing on power electronics, cyber-physical systems, and renewable energy.

Sukumar Mishra received the M.Tech. and Ph.D. degrees in electrical engineering from the National Institute of Technology, Rourkela, India, in 1992 and 2000, respectively. He was associated with IIT Delhi as a Professor, and has been its part for the past 20 years and currently working as The Director at Indian Institute of Technology (ISM), Dhanbad, India. He is the founder of Silov Solutions Private Limited, a company that specifically deals in products related to renewable energy sources utilizable at household scale as well as at commercial setups. He has been granted fellowships from academies like NASI (India), INAE (India), and professional societies like IET (U.K.), IETE (India), and IE (India). He has also been recognized as the INAE Industry Academic Distinguished Professor.

Abdelkader El Kamel received the Engineering Diploma, master's Diploma, and Ph.D. degree from Centrale Lille Institute, Villeneuve-d'Ascq, France, where he is currently a Professor. He is also a regular Visiting Professor to China, Mexico, Tunisia, and Chile and an Expert for various international organizations. His main research interests include intelligent systems monitoring, complex systems analysis and control, computational intelligence, and optimization. Applying intelligent technologies, virtual reality, and optimization techniques in transportation systems and mobile cooperative robots are among the current focuses of his work. In 2017, he was the recipient of the Highest Research Distinguished Evaluation AAA.